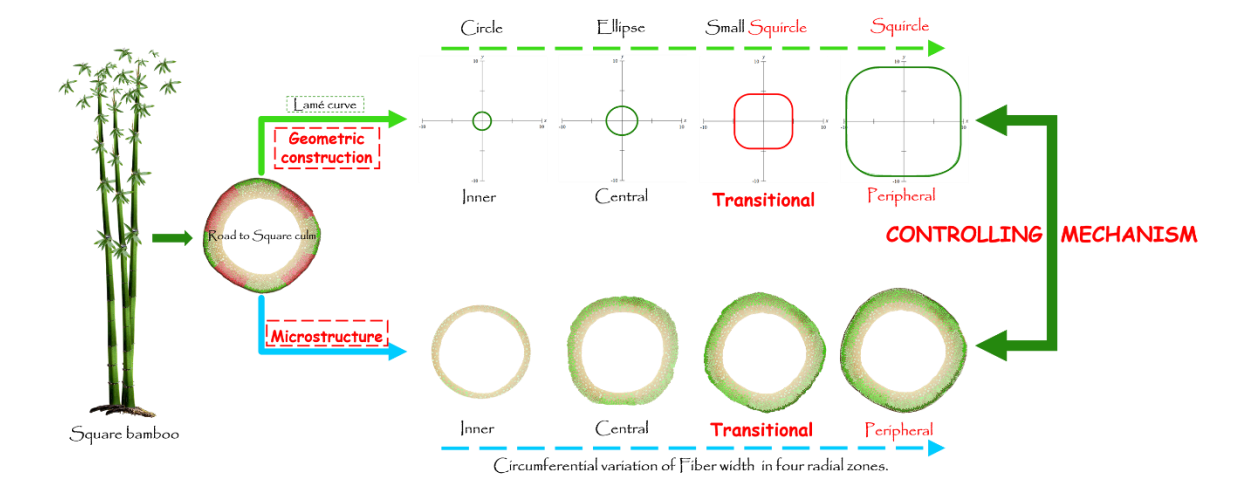
Interactions between Geometrical Forms and Microstructural Features in Culm of Square Bamboo

Qianqian Jiang, a,b,f Wenli Gao, a,f Zhangchao Ding, Changqing Lu, a,f Yan Yan,d Min Yu, a,f Junlan Gao,d Liang Zhou, a,f,* and Shengquan Liu a,f,*

DOI: 10.15376/biores.19.4.8894-8911

GRAPHICAL ABSTRACT



^{*} Corresponding authors: mcyjs1@ahau.edu.cn; liusq@ahau.edu.cn

Interactions between Geometrical Forms and Microstructural Features in Culm of Square Bamboo

Qianqian Jiang, a,b,f Wenli Gao, a,f Zhangchao Ding,c Changqing Lu,a,f Yan Yan,d Min Yu,a,f Junlan Gao,d Liang Zhou,a,f,* and Shengquan Liu a,f,*

Bamboo culms can alter the bamboo's geometric shape by adjusting the hierarchical organization of anatomical components as a means of adapting to different living conditions. Therefore, a square-like culm has been found commonly in the Chimonobambusa bamboo species. However, the underling mechanism for how these anatomical components assemble into a square culm in the species remains to be considered. Furthermore, the relationship between the geometrical construction of culm and its corresponding organization of anatomical components within also needs clarification. Therefore, the geometrical construction of crosssections was examined in this work. A super-ellipse based on the Lamé curve was confirmed. Additionally, the transitional zone, at 3/4 in the radial direction, was detected as an inflection point where the geometric parameters clearly changed. Meanwhile, anatomical observation also suggested that the transitional zone can be identified as an inflection point because the fibre morphology difference in circumferential regions becomes more apparent in this area. It is worth mentioning that there is a coherence between the geometrical and microstructural features in circumferential and radial variation. These findings are meaningful to manifest the controlling mechanism of hierarchical structures on the geometrical shape of bamboo culm.

DOI: 10.15376/biores.19.4.8894-8911

Keywords: Square bamboo; Geometrical constructions; Morphological properties of fibre; Variation patterns

Contact information: a: Anhui Agricultural University, 130 Changjiang West Road, Hefei 230036, P.R. China; b: Bozhou University, 2266 Tangwang Avenue, Bozhou 236800, P.R. China; c: Guizhou Forestry School, 380 Qianjin South Road, Guiyang 550201, P.R. China; d: International Centre for Bamboo and Rattan, Beijing 100102, PR. China; e: Anhui Academy of Agricultural Sciences, 40 Nongke South Road, Hefei 230001, P.R. China; f: Key Lab of State Forest and Grassland Administration on "Wood Quality Improvement & High Efficient Utilization", 130 Changjiang West Road, Hefei 230036, P.R. China; * Corresponding authors: mcyjs1@ahau.edu.cn; liusq@ahau.edu.cn

INTRODUCTION

In the natural world, the beauty of plant diversity is in part from the natural shapes of flowers, leaves, and culms. The culm of the most common plants has the form of a cylinder. However, compared with the circular shape, the square culm has shown a formidable talent for control of its morphology. Unique square culms are exhibited by some Lamiaceae, Melastomataceae, or some species of Bambusoideae (Van Oystaeyen *et al.* 1996; Gielis 2003, 2017). One of the most glaring examples is *Chimonobambusa* from Bambusoideae, which has been elucidated for a long history of morphological, anatomical, and ecological aspects (Dyer 1885; Li and Chin 1960; Gielis 2003; Lou *et al.* 2021).

Notably, Dyer (1885) proposed the name *Chimonobambusa quadrangularis*. The plant has noticeably four-angled culms and named it square bamboo in earlier studies. *Chimonobambusa utilis* is generally distributed in Guizhou, Yunnan, and Sichuan regions of China, presenting a typical square-like culm (Shi 2017), which had been used traditionally in the pulp and paper and biochar industry (Zhu and Yao 1964; Liu *et al.* 2018). Additionally, its square shape with rounded corner structure is also widely used in aeronautic and aerospace engineering due to its good performance in crashworthiness (Chen *et al.* 2017, 2021). Further, it is well accepted that the geometrical construction and microstructures are closely associated with plant culm type (Gielis 2017; Jiang 2020). Therefore, research on square bamboo culm is essential to understand the mechanism of how to manipulate the geometrical shape of culm. Furthermore, it is also meaningful to increase the economical benefits of the bamboo species.

The anatomical structures of a bamboo culm in cross-section are characterized by vascular bundles and parenchyma tissue (Grosser and Liese 1971). Fibres were characterized by the elongated form and frequently forked ends, which appeared as sheaths of vascular bundles in monopodial bamboo (Liese 1987). Differences in fibre length (Yue et al. 2017; Wang et al. 2018; Chen et al. 2018), fibre width (Chen et al. 2018), and fibre cell wall thickness (Yang 2020) have affected the variation in culm (Liese and Köhl 2015). Thus, the morphology of various anatomical components and its corresponding variation pattern in the square culm have been studied. The earliest research on the Chimonobambusa described anatomical and morphological characteristics of rhizome-root (Takeuchi 1932). The type (Li and Chin 1960) and structure (Li et al. 1962) of vascular bundles, fibre form, and its application (Zhu 1964) were examined. Recently, significant variations in fibres from the radial and axial direction were reported (Lin 2004), and circumferential variation of anatomical structures also is present in Chimonobambusa quadrangularis (Jiang et al. 2021). These findings described the structure of the squarelike culm at a microscopic level, but the comprehensive analysis of circumferential and radial variation patterns was not well illustrated (Jiang et al. 2021). Meanwhile, ongoing investigation on the shape of square bamboo is beyond simple visual description. Geometrical construction was applied to manifest the culm shape of square bamboo (Gielis 2017). Square-like culms were also confirmed in *Chimonobambusa utilis* using modelling large-scale empirical data obtained from scanned cross-sections (Huang et al. 2020). However, the transitional pattern from externally square and internally round in the crosssection of square culm have not been discussed, especially in combination with the related mathematical models (Jiang et al. 2021). Furthermore, the relationship between microstructural features and geometrical constructions in those square-like culms remains to be discussed.

To explore related factors involved in the formation of the square culm, the radial variation of geometrical constructions was analysed using a mathematical approach. The microstructure of the square culm cross-section were observed by stereomicroscope, and then the circumferential differences of microstructural characteristics at different radial positions were calculated. Coherence of variation pattern between anatomical characters and geometrical constructions were verified for investigating the inherent relationship between macroscopical shape of culm and microscopical organization of anatomical components. These results will provide important information to understand to how the bamboo species alter its hierarchical structures to realize a special shape of culm for

meeting a certain living requirement. It also could be useful for exploring other effective utilizations than pulping and biochar for the bamboo species.

EXPERIMENTAL

Materials

Materials for this investigation were collected in Tongzi, Guizhou, China, in which *Chimonobambusa utilis* is naturally distributed. Three groups of bamboo (n-1, n-2, and n-3; Fig. 1) were harvested, and each group of bamboo was divided into three sections individually according to the different positions of the base, middle, and top. All of the specimens had a squarish shape. The culm diameter at chest height of n-1, n-2, and n-3 was 12.18 mm, 11.03 mm, and 7.82 mm, respectively. And the average cross-section thickness of the culm wall of n-1, n-2, and n-3 was 1.82 mm, 1.64 mm, and 1.41 mm, respectively. The habitat and morphological characteristics of the samples are presented in Table 1 (the figures referred to Tongzi county forestry station).



Fig. 1. Non-treated samples

Table 1. Habitat and Description of *Chimonobambusa utilis*

Com	Desc	cription				ŀ	Habitat			
Sam ples	H (m)	Age (year)	AS	AMT (o C)	RH (%)	AAP (mm)	FFP (days)	Altitude (m)	MASD (h)	LL
n-1	2.07	2	Shady							106°
n-2	3.28	3	67.8°-	,	4 79	1434	150-	2800	1091.6	26'E,
n-3	3.78	4	83.5°				270			27°5 7′N

H = height, CD = culm diameter at chest height, CT = the average cross-section thickness of the culm wall, AS = aspect and slope, AMT = annual mean temperature, RH = relative humidity, AAP = annual average precipitation, FFP = frost-free period, MASD = mean annual sunshine duration, and LL = latitude and longitude

Circumferential Differential Method

The cross-sections of the culm presented like a square, exhibiting a four-angled structure. According to the authors' previous study, the sharper edges were marked as the 'corner region' (c) and the flatter edges were marked as 'side region' (Jiang *et al.* 2021). Therefore, cross-sections of square culm were separated into eight continuous subzones

(Fig. 2). Furthermore, based on the measurement of culm wall thickness at circumferential position (Table S1), each circumferential zone was divided into four subzones, namely peripheral, transitional, central, and inner according to the arrangement of vascular bundles (Fig. 2) (Grosser and Liese 1971). Therefore, in total 32 subzones were allocated at a cross-section of square culm, and they were numbered as listed in Table S1 for consequently analysing the variation of geometrical constructions and anatomical structures (Table S1). Even the thickness of culm varies at different single bamboo, the transitional zone was generally located at 3/4 in the radial direction.

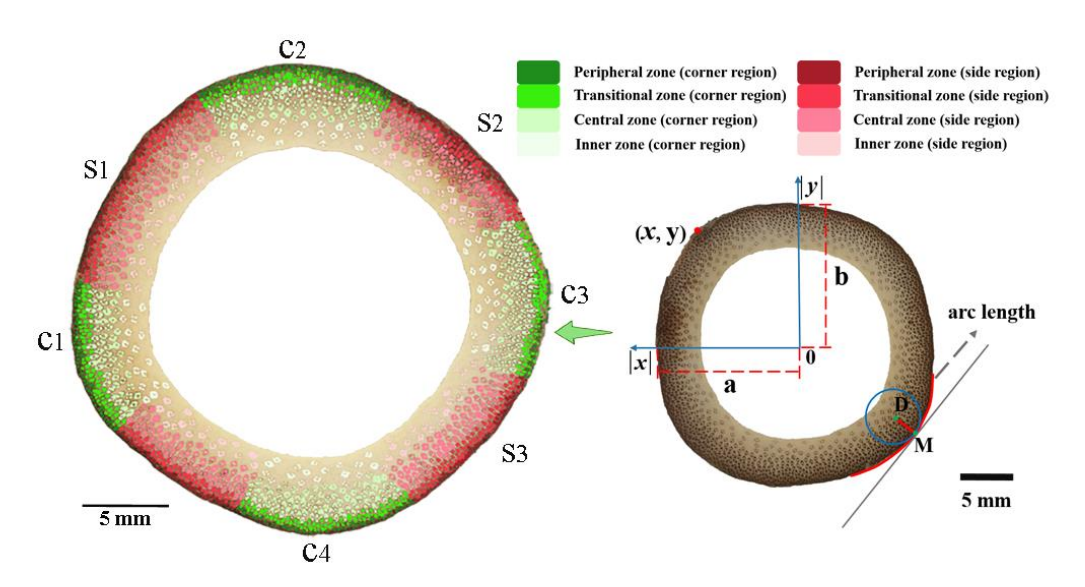


Fig. 2. Illustration of circumferential and radial regions in cross-section; a: the half length of the long axis, b: the half length of the short axis; D: the centre of the maximum osculating circle on the curve; M: the point that the normal is perpendicular to the tangent on a curve; |DM|: the radius of the curvature, namely radius of maximum osculating circle at a certain point of the curve

Geometric Analysis

The radius of curvature is mainly used to describe the degree of bending changes at a certain point on a curve (Gielis 2003). |DM| denotes the radius of the curvature, namely radius of maximum osculating circle at a certain point of the curve (Fig. 2). D denotes the centre of the maximum osculating circle on the curve, M denotes the point that the normal is perpendicular to the tangent on a curve (Gielis 2003). To detect the flexibility of curves at the subzone, the curves were taken at equal length (1/8 length of circumference). The measurement of radius of the curvature were executed by Image J software (National Institutes of Health, Jv1.53t, Bethesda, MD, USA).

Additionally, the lamé curve can be used to determine the shape of circles, squares, astroids, ellipse, superellipse, hyporellipse, hyporellipse, and a whole family of curves and surfaces (Lamé 1818; Gielis 2017). The lamé curve is the set of points satisfying the following Eq. 1 described as follows:

$$\left|\frac{y}{a}\right|^n + \left|\frac{y}{b}\right|^n = 1\tag{1}$$

As presented in Fig. 1, in Cartesian coordinate system, x and y denote value of coordinate point, 2a denotes the length of long axis, 2b denotes the length of short axis, n denotes exponent (Lamé 1818). Typical types of the superellipse were settled according to

the formula. When a = b, n = 2, the (super) ellipses become (super) circles. If $a \neq b$, for n = 2, the superellipse resembles ellipse; for n > 2, the superellipse is known as hyperellipse; for n = 4, the superellipse resembles a squircle (Lamé 1818; Gielis 2017). Typical types of superellipse shapes are shown as below (Fig. 3).

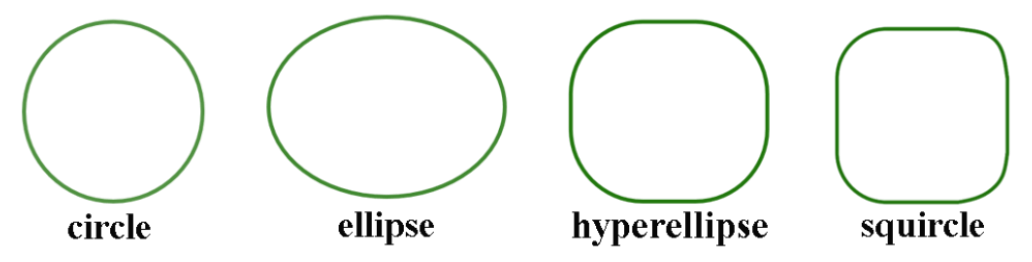


Fig. 3. Typical types of the superellipse

Therefore, the formula was used to clarify the geometrical constructions of square culm of bamboo, Values of 'a', 'b', 'x', and 'y' were measured by Image J software based on the scale bar, and then 'a', 'b', 'x', and 'y' were plugged into the equation, the value of n was subsequently calculated. After that, Grafeq software (Pedagoguery Software Inc., 2.1.2, Terrace, Canada) was utilized to predict geometry of superellipse based on those measured and calculated parameters, and then corresponding fitting-figures were depicted (Goulart 2009).

Microscopy Observation and Image Analysis

To determine the variation patterns of anatomical structures, every fourth internode was obtained starting from the base to the top of each bamboo (Gross and Liese 1971). Altogether, nine internodes from three culms of *Chimonobambusa utilis* were evaluated in this work. Each internode was cut into 3-cm-thick ring-like tubes, and then cross-sections of 15 μ m thickness could be obtained using a Lycra Slicer (Leica RM2265) after being softened in 80 °C water bath for 8 days. A total of 60 individuals were measured for fibre wall thickness (WT) and fibre width (FW), and number of vascular bundles within a certain range (1 mm \times 1 mm, 0.5 mm \times 0.5 mm) (DVBs) were counted at each subzone.

All slices were examined under an HD Stereo Digital Microscope (KEYENCE VHX-600E) (Rúgolo 2003). Furthermore, bamboo culm was cut into matchstick-shaped battens based on each subzone and incubated at 80 °C for 4 h after being infused with 31.3% hydrogen peroxide and 99.8% glacial acetic acid at a ratio of 1:1 to adequately separate the single fibres for measurement (Groom *et al.* 2002a) (Burgert *et al.* 2005). The 60 individuals were measured for the length (FL) at each subzone.

Statistical Analysis

To compare the circumferential and radial variation of the anatomical structures, FL, FW, WT, and DVBs were measured and counted at each subzone using ImageJ software (National Institutes of Health, Jv1.53t, Bethesda, MD, USA). Arrangement of vascular bundles were observed by HD Stereo Digital Microscope. A one-way (ANOVA) test was performed for exploring variation patterns as follows,

$$F = \frac{MSG}{MSE} \tag{2}$$

where SSR is the regression sum of squares, SSE is the error sum of squares, and SST is the total sum of squares (SST = SSR + SSE). In addition, dfr is the regression degrees of freedom (dfr = k-1), dfe is the error degrees of freedom (dfe = n-k), dft is the total degrees of freedom (dft = n-1), k is the total number of groups, k is the total observations, MSR is the regression mean square (MSR = SSR/dfr), MSE is the error mean square (MSE = SSE/dfe), k is the k test statistic (k = MSR/MSE), and k is the k-value that corresponds to k-fdfr, dfe.

RESULTS AND DISCUSSION

Variation in Geometric Features

The radius of curvature is an important parameter to reflect the degree of curves deviation from a straight line (Gielis 2017). The measurements of geometrical parameters are listed in Table 2. From Table 2, |DM| at the corner and at side region was different from each other. For example, in n-3, it was 2.32 and 0.24, respectively. It is generally accepted that the greater the radius of curvature, the sharper the edges, whereas the smaller the radius of curvature, the flatter the edges (Lamé 1818). Therefore, it means that geometry of square culm varied between different single bamboo, and there were also differences of geometry between the corner and side region of single bamboo culm. Therefore, the value of |DM| provides a reference value of geometry of square culm and make the comparison among shape of different samples more convenient and precise than only using descriptive words. In addition, it is found that the value of |DM| changes at different radial position in same circumferential region. Generally, it decreased from the inner to the peripheral. It indicates that both inner and central zone deviated further from straightness than the transitional and peripheral zone did.

Table 2. Measurements of Radius of Curvature Parameters

		nferential gion		Radial zone	(Side Direction	n)
Sample	Corner	Side	Inner	Central	Transitional	Peripheral
	DM (mm)	DM (mm)	DM (mm)	DM (mm)	DM (mm)	DM (mm)
n-1	1.13	0.26	1.01	1.00	0.26	0.26
n-2	1.16	0.35	0.89	0.88	0.36	0.35
n-3	2.32	0.24	1.28	1.28	0.24	0.24

|DM|: radius of curvature

To illustrate the radial variation of geometric features more precisely, the Lamé curve was utilized here since it was used to measure distances and define the geometry of surfaces (Lamé 1818). Therefore, the Lamé curve was used to examine the geometrical constructions of square culm for clarifying the radial difference of the cross-section. By adding the present measurements of the square culm into the formula of the superellipse, the results are listed in Table 3. Take n-3 as an example, in the inner zone, a = b, n = 2, it fits close to the circular data. In the central zone, the value of a was approximately equal to b, n = 2, it fits close to the ellipse data. In the transitional zone, $a \neq b$, a = 13.58, b = 12.10, n = 4, it fits close to the squircle data. In the peripheral zone, $a \neq b$, a = 14.04, b = 12.75, n = 4, it fits also close to the squircle data (Table 3). These implied that the geometric

parameters of all subzones fit the superellipse data, and the transitional zone, namely at 3/4 in the radial direction, was the inflection point where the parameters of superellipses have changed. Therefore, Lamé curve was used to examine the geometrical constructions of square culm for clarifying the radial difference of the cross-section, and the inflection point has been identified at the transitional zone.

		Per	ipheral		Transitional			Central			Inner		
	Sample	a (mm)	b (mm)	n	a (mm)	b (mm)	n	a (mm)	b (mm)	n	<i>a</i> (mm)	b (mm)	n
	n-1	13.40	12.39	4	12.98	11.76	4	11.26	11.14	2	9.08	9.08	2
	n-2	13.49	12.51	4	13.03	12.10	4	10.46	10.41	2	9.17	9.16	2
	n-3	14.04	12.75	4	13.58	12.10	4	10.24	10.21	2	9.41	9.41	2

Table 3. Measurements of Superformula Parameters

2a =the length of long axis, 2b =the length of short axis, n =exponent

Variation in Microstructures

The vascular bundles are usually regarded as one of the most important anatomical characteristics of the bamboo (Grosser and Liese 1971). To evaluate the circumferential variance of the microstructures between the corner and side regions, the morphology of vascular bundles was observed. The results showed that the vascular bundles exhibited an 'undifferentiated' appearance in the peripheral zone, displayed a 'semi-differentiated' appearance in the transitional zone, and presented as an 'open' appearance in the central and inner zone (Figs. 4 and 5) (Grosser and Liese 1971).



Fig. 4. The anatomical structures of the corner A) and side regions B) in the cross-section

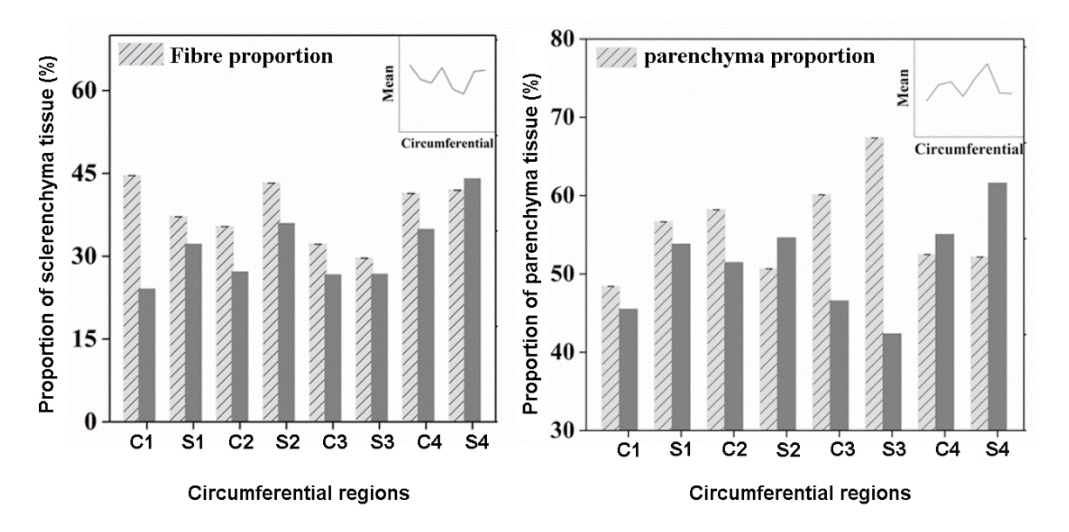


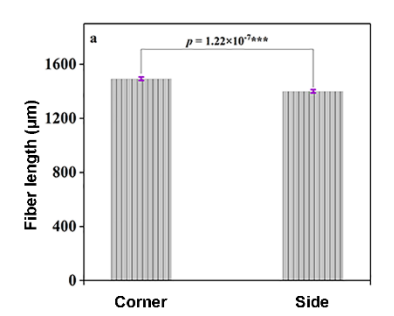
Fig. 5. Difference of tissue proportions in circumferential regions

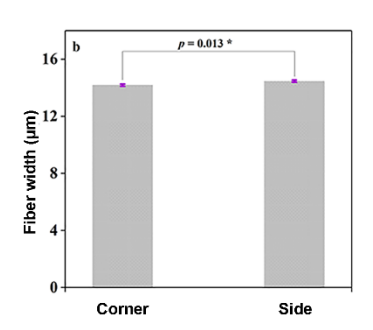
These findings suggest that the vascular bundles display the same characteristics both at the corner and side regions. The findings indicated that there was no circumferential difference in the arrangement and distribution of the vascular bundles across the culm wall, as well as the tissue proportions. Fibre is the main anatomical component in vascular bundles, and its morphology varies at different positions in culm (Li and Chin 1960). To compare the characteristics of fibre between the corner and side regions, fibre length (FL), fibre width (FW), and fibre wall thickness (WT) were measured at each circumferential micro region, and the results are listed at Table S2. The measurement showed that value of FL was 1402.4 to 1591.9 μm, FW was 13.5 to 15.6 μm, and WT was 13.2 to 14.0 μm. These measured values resemble the reported works in *Chimonobambusa quadrangularis* from same genera (Lin 2004). Furthermore, analysis of radial variation was generally performed to clarify the variation patterns of anatomical structures in bamboo. The results in the present work showed a significant difference of all measured characteristics in radial direction (Table S2). A similar radial variation pattern was also depicted in the previous reported work (Lin 2004). Unfortunately, comparison of fibre morphology among circumferential regions has not been involved in the previous study (Lin 2004). The current authors found that fibre morphology changes at different circumferential regions. Take n-3 for example, the average value of FL was 1492.36 µm at corner region and 1402.40 µm at side regions. As shown in Fig. 6, the ANOVA result indicates that the difference of FL between the corner and side region was significant at 0.001 levels. Moreover, the difference of FW was significant at 0.05 levels and the difference of WT was significant at 0.01 levels. The results suggest a significant difference between corner and side region, and fibres at corner regions presented longer and thinner than those of the side regions.

Table 4. Measurement of Parameters of Fibre Morphology

Samples	FL (um)	FW	(µm)	WT (µm)	
Samples	С	S	С	S	С	S
n-1	1591.9	1512.9	15.2	15.6	11.9	13.4
n-2	1585.9	1585.3	13.5	13.6	13.3	13.5
n-3	1492.6	1399.4	14.2	14.5	11.9	12.8

FL = fibre length, FW = fibre width, WT = fibre wall thickness, C = corner regions, S = side regions





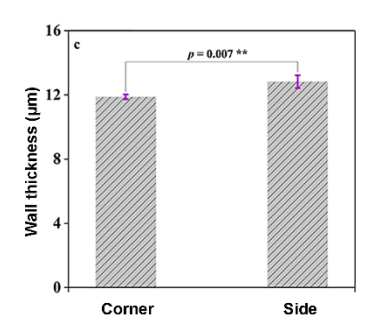


Fig. 6. The circumferential variation in fibre characteristics. P-values were calculated using Kruskal–Wallis non-parametric analysis of variance. For each parameter, significance was indicated as follows: * p < 0.05, ** p < 0.01, and *** p < 0.001

It should be noticed that fibre morphology not only changes with different radial positions but also with circumferential regions. Under such circumstances, it is difficult to draw a consistent circumferential variation pattern of fibre morphology at different radial position. For example, the location of radial maximum of FW is different between the corner and side region (Fig. 7). In the purpose of comparing fibre morphological characters between circumferential positions more clearly, one way ANOVA was performed at each radial zone. The results show that the significant difference of FW, WT, and DVBs was not detectable both at inner zone and central zone. Nevertheless, the difference of DVBs and WT changed into significant from transitional zone to peripheral zone. The findings indicate that the difference of fibre morphology and density of vascular bundles between core side and edge side become more apparent from the transitional zone (Fig. 8). These findings possibly suggest that an inflection point of the difference can be identified at the transitional zone.

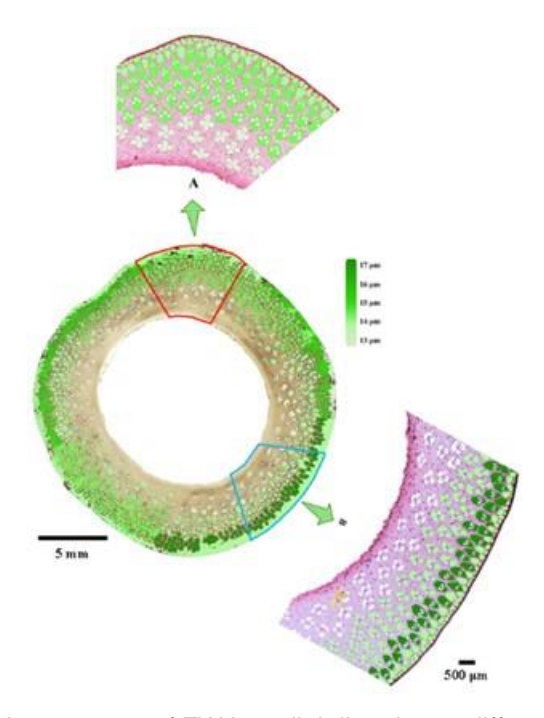
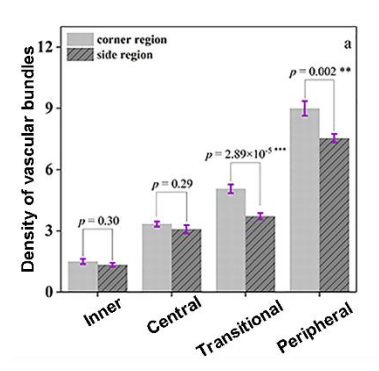
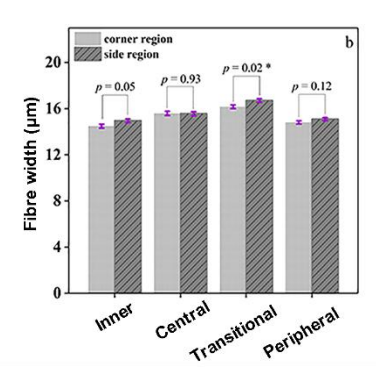


Fig. 7. Illustration of variation patterns of FW in radial direction at different circumferential position: A) Radial variation patterns of FW in corner region, B) Radial variation patterns of FW in side region





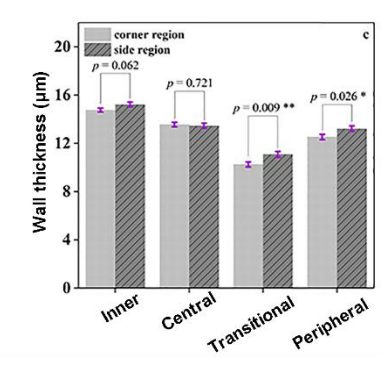


Fig. 8. The circumferential variance analysis of anatomical characteristics at each radial subzone. A) Variance analysis of density of vascular bundles. B) Variance of fibre width. P-values were generated using Kruskal–Wallis non-parametric analysis of variance. For each parameter, significance was indicated as follows: *p < 0.05, **p < 0.01, and ***p < 0.001.

Comprehensive Analysis of Geometrical Construction and Microstructure

Chimonobambusa quadrangularis was named as 'square bamboo' on account of its 'four-angled' culm (Dyer 1885). It is well known that bamboo culms can alter its geometric shape by changing anatomical structures (Jiang 2020). Therefore, the interactions between geometrical constructions and anatomical structures are worthy of investigating, and it helps to understand the mechanism of how the bamboo change its microstructure to realize a required geometrical construction of culm.

As mentioned already, the Lamé curve demonstrated that the geometrical constructions of 'four-angled' culms fit the superellipse data well (Table 2). Furthermore, Grafeq software, which is based on Lamé curve, is capable of depicting a fitting-figures of superellipse according to measured and calculated parameters (Goulart 2009). Therefore, the Lamé curve can be used to describe the variation patterns of geometrical constructions at different radial zones. It is found that parameters of the superellipse change successively from the inner to peripheral in the square culm (Fig. 9). The transitional zone was detected as the inflection point where the geometrical constructions transformed. Meanwhile, anatomical observation also suggested that the transitional zone can be identified as an inflection point because the difference of fibre morphology and DVBs between core side and edge side become more apparent from here.

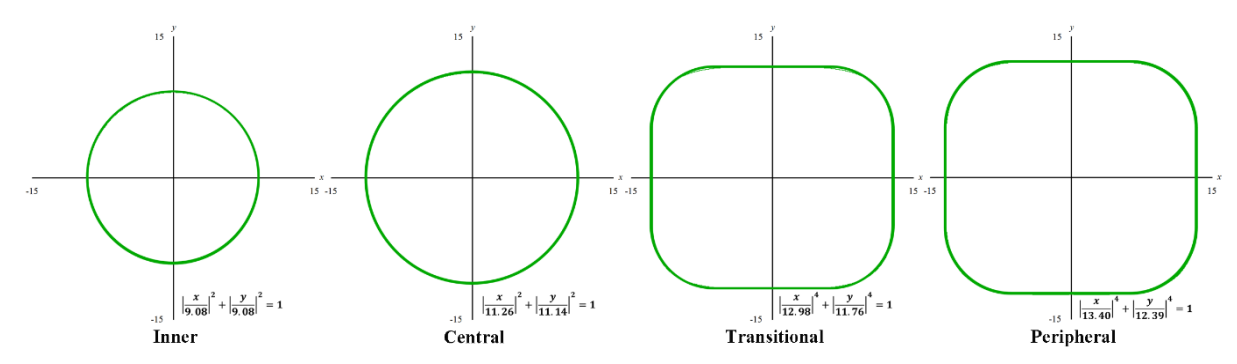


Fig. 9. Radial variation pattern of geometrical constructions of sample n-1 cross-section

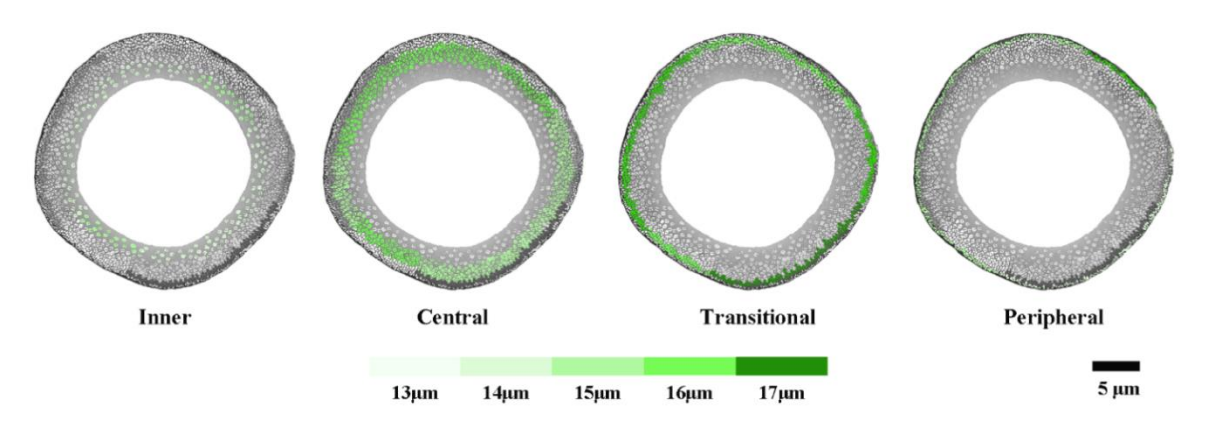


Fig. 10. Circumferential variation patterns of the FW at different progressive radial zone. Scale bar: $5 \mu m$, colour scale: Fibre width

It is interesting to find this coherence between the geometrical and microstructural features in circumferential and radial variation (Fig. 10). To some extent, it explains how the bamboo "modulate" its anatomical components to build a required geometrical construction of culm. Radial variation of DVBs and fibre morphological parameters, especially WT, can become steeper in corner side than the edge side when the radial position close to the transitional zone, namely around 3/4 in the radial direction. This difference may cause the geometry of the culm to change to a superellipse.

The morphology that was square externally and round internally performed better than circular and square structure in aseismic behaviour, stiffness (Chen et al. 2017), impact resistance and stability (Chen et al. 2021), and ultimate bearing capacity based on available data (Orangi et al. 2011; Zheng et al. 2016), related to space use or resistance against bending or torsion (Gielis 2003). Moreover, such structures can improve transverse tensile strength, and prevent the bamboo from expansion and splitting, while sustaining the varied environmental load bearing wind, snow, and gravity (Gielis 2003; Chen et al. 2021). Such evolution can allow the beneficial effects of inheritance or development (Gielis 2017). Previous studies showed that variation of FL and FW was related to the change of culm type between Phyllostachys edulis and its variety Phyllostachys edulis f. tubaeformis (Yue et al. 2017). Change of FW and WT was related to culm type differentiation in Dendrocalamus sinicus (Guo 2018). Further, FW was significantly correlated with the difference of culm type between Phyllostachys edulis and its variety Phyllostachys edulis 'Pachyloen' (Yang 2020). The *Chimonobambusa utilis*, used in the present work, grow at heights between 1200 to 2800 m of altitude, with slope of 67.8° to 83.5°. This might pose a situation where the bamboo must change the structure to adapt to steeper grades in the natural distribution plateau regions, which may be available by morphological changes in fibres. Taken together, these results suggest that changes of fibre morphology and vascular bundles distribution at the transitional zone might be associated with the formation of square-like culm. The sclerenchyma fibre cell can bear mechanical actions with small lumen diameter and thick cell walls (Grosser and Liese 1971). Additionally, the inflection point was identified at the transitional zone where the geometrical and anatomical structures transformed (Figs. 9 and 10). This is probably because the vascular bundles displayed as semi-differentiated in the transitional zone, which were unable to maintain a stable form (Grosser and Liese 1971).

CONCLUSIONS

Square bamboo has typical 'four-angled' culms. Geometrical constructions and anatomical structures of the culm were rigorously investigated in order to reveal the interactions between them. The results suggested that:

- 1. The transitional zone in the radial direction was the inflection position where the geometrical constructions of cross-sections were transformed to a squircle.
- 2. The transitional zone also was identified as an inflection point where radial variation of vascular bundles and fibre morphological parameters is steeper in corner side than the edge side.
- 3. The coincidence between geometrical constructions and anatomical structures of cross-sections was established.
- 4. The bamboo manipulates its morphology, with respect to fibres and DVBs, to realize a required shape of culm. Based on the living conditions of *Chimonobambusa utilis*, it hypothesized that this bamboo species organized its anatomical component in a special way to build a squircle externally and round internally culm for adapting the high latitude and steeper land in its natural distribution.

ACKNOWLEDGMENTS

The corresponding authors contributed equally to this article. The authors would like to thank the School of Forestry and Landscape Architecture, Anhui Agricultural University for assisting in microscopy and Key Lab of State Forestry and Grassland Administration on Wood Quality Improvement & High Efficient Application, and Key Lab of Wood Science & Technology of Anhui Province for providing laboratory facilities. This research was financially supported by L.S.Q. acknowledge funding of the sub-task of the national "13th Five-Year" key research and development plan on the Properties of Round **Spliced** Bamboo and Design and Manufacture of Modular (2016YFD060090502), J.Q.Q. acknowledge funding of Anhui Agricultural University "Study on the Formation Mechanism of Square bamboo" (2021yis-9) and Natural Science Foundation of Anhui Province "The formation mechanism of variational cell wall structural in Square bamboo based on lignin biosynthesis pathway" (YJS20210214), Y.Y. acknowledge funding of Fundamental Research Funds of ICBR (No. 1632020010). As well as Y.M. acknowledge funding of "National Natural Science Foundation of China (Grant No. 31800475) and Natural Science Foundation of Anhui Province (Grant No. 1908085QC111)".

REFERENCES CITED

Burgert, I., Frühmann, K., Keckes, J., Fratzl, P., and Stanzl-Tschegg, S. (2005). "Properties of chemically and mechanically isolated fibres of spruce (*Picea abies* [L.] Karst.). Part 2: Twisting phenomena," *Holzforschung* 59(2), 247-251. DOI: 10.1515/HF.2005.039

- Chen, M., Zheng, L., Zheng, Y., and Lin, Z. (2017). "Research on flexural behaviour of curved concrete filled steel tubular members," *Steel Construction* 32(09), 52-56. DOI: 10.13206/j.gjg201709010
- Chen, L., Guo, X., Cui, Y., Zheng, X., and Yang, H. (2018). "Comparative transcriptome analysis reveals hormone signaling genes involved in the launch of culm-shape differentiation in *Dendrocalamus sinicus*," *Genes* 9(1), article 4. DOI: 10.3390/genes9010004
- Chen, X., Ma, B., and Chen, Y. (2021). "Analysis and optimization of crashworthiness of the thin-walled tube based on the square bamboo structure," *Journal of Machine Design* 38(5), 78-84. DOI: 10.13841/j.cnki.jxsj.2021.05.008
- Dyer, W. (1885). "The square bamboo," Nature 32, 391-392. DOI: 10.1038/032391d0
- Gielis, J. (2003). "A generic geometric transformation that unifies a wide range of natural and abstract shapes," *American Journal of Botany* 90(3), 333-338. DOI: 10.3732/ajb.90.3.333
- Gielis, J. (2017). *The Geometrical Beauty of Plants*, Atlantis Press, Paris, France. DOI: 10.2991/978-94-6239-151-2
- Goulart, J. (2009). "O estudo da equação ax²+by²+cxy+dx+ey+f=0 utilizando o software Grafeq: uma proposta para o ensino médio [The study of the equation Ax²+By²+Cxy+Dx+Ey+F=0 using the Grafeq software: A proposal for high school]," *Programa de Pós-Graduação em Ensino de Matemática*. http://www.peda.com/grafeq/
- Groom, L., Mott, L., and Shaler, S. (2002). "Mechanical properties of individual southern pine fibres. Part I. Determination and variability of stress-strain curves with respect to tree height and juvenility," Wood and Fibre Science 34(2), 221-237. DOI: 10.1007/s004680100123
- Grosser, D., and Liese, W. (1971). "On the anatomy of Asian bamboos with special reference to their vascular bundles," *Wood Science and Technology* 5(4), 290-312. DOI: 10.1007/BF00365061
- Huang, W., Li, Y., Niklas, K., Gielis, J., Ding, Y., Cao, L., and Shi, P. (2020). "A superellipse with deformation and its application in describing the cross-sectional shapes of a square bamboo," *Symmetry* 12(12), article 2073. DOI: 10.3390/sym12122073
- Jiang, Q., Ding, Z., Lu, C., Gao, J., Yan, Y., and Liu, S. (2021). "Anatomical characterization of *Chimonobambusa quadrangularis* based on circumferential and radial variation patterns in cross-sections," *IAWA Journal* 43(1-2), 164-177. DOI: 10.1163/22941932-bja10071
- Jiang, Z. (2020). "Research advances in bamboo anatomy," *World Forestry Research* 33(3), 1-6. DOI: 10.13348/j.cnki.sjlyyj.2020.0036.y
- Lamé, G. (1818). Examen des Diérentes Méthodes Employées pour Résoudre les Problèmes de Géométrie [Examination of Different Methods Used to Solve Geometry Problems], Courcier, Paris, France.
- Li, D. (2008). "Radius of curvature," in: *Encyclopaedia of Microfluidics and Nanofluidics*, Springer, Boston, MA, USA, pp. 1171. DOI: 10.1007/978-0-387-48998-8
- Li, Z., and Chin, Z. (1960). "Anatomical studies of some Chinese bamboos," *Journal of Integrative Plant Biology* 9(1), 76-97.

- Li, Z., Chin, Z., and Yao, X. (1962), "Further anatomical studies of some Chinese bamboos," *Journal of Integrative Plant Biology* 10(1), 15-28.
- Liese, W. (1987). "Research on bamboo," *Wood Science and Technology* 21, 189-209. DOI: 10.1007/BF00351391
- Liese, W., and Köhl, M. (2015). *Bamboo-The Plant and its Uses*, Springer, Cham, Switzerland. DOI: 10.1007/978-3-319-14133-6
- Lin, J., Lin, Y., Lai, G., and Dong, J. (2004). "A study on the law of variation in fibre morphology of *Chimonobambusa quadrangularis* Culm-wood," *Journal of Acta Agriculturae Universitatis Jiangxiensis* 26(01), 56-58.
- Liu, W., Zhang, L., Cui, X., Li, W., Zhang, W., and Wang, Y. (2018). "Pyrolysis of *Chimonobambusa utilis* (Keng) Keng F. and characteristics of its carbonization products," *Journal of Bamboo Research* 37(3), 85-92.
- Orangi, S., Abrinia, K., and Bihamta, R. (2011). "Process parameter investigations of backward extrusion for various aluminum shaped section tubes using FEM analysis," *Journal of Materials Engineering and Performance* 20, 40-47. DOI: 10.1007/s11665-010-9655-8
- Rúgolo, D., and Rodríguez, M. (2003). "Culm anatomy of native woody bamboos in argentina and neighboring areas: Cross section," *Bamboo Science & Culture: Journal of the American Bamboo Society* 17, 28-43.
- Shi, J., Zhang, Y., Zhou, D., Ma, L., and Yao, J. (2017). "A review of bamboo cultivar from *Chimonobambusa* in the world," *World Bamboo and Rattan* 15(06), 41-48. DOI: 10.13640/j.cnki.wbr.2017.06.012
- Takeuchi, O. (1932). Study on Bamboo, Youkendou, Japan.
- Van Oystaeyen, F., Gielis, J., and Ceulemans, R. (1996). "Mathematical aspects of plant modelling," *Scripta Botanica Belgica* 13, 7-27.
- Wang, T., Liu, L., Wang, X., Liang, L., Yue, J., and Li, L. (2018). "Comparative analyses of anatomical structure, phytohormone levels, and gene expression profiles reveal potential dwarfing mechanisms in shengyin bamboo (*Phyllostachys edulis* f. *tubaeformis*)," *International Journal of Molecular Sciences* 19(6), article 1697. DOI: 10.3390/ijms19061697
- Yang, B., Shen, Z., Li, Z., Li, Y., Shen, X., and Chen, Y. (2020). "A study on the stalk factor and fibre traits and their correlation of *Phyllostachys edulis* 'Pachyloen'," *Acta Agriculturae Universitatis Jiangxiensis* 42(1), 101-109.
- Yue, J., Yuan, N., and Peng, Z. (2017). "Preliminary studies on culm type variation and ideal culm type in bamboos," *Journal of Bamboo Research* 36(02), 49-56.
- Zheng, Y., He, C., and Zheng, L. (2016). "Flexural behaviour and practical calculation of load bearing capacity for composite sectioned square concrete filled steel tube reinforced by inner circular steel tube," *Building Science* 32(05), 34-38.
- Zhu, H., and Yao, X. (1964). "Studies on the fibre structure of 33 Chinese bamboos available for pulp manufacture," *Journal of Science of Forestry* 10(4), 311-331.

Article submitted: November 5, 2023; Peer review completed: February 3, 2024; Revised version received: June 25, 2024; Accepted: September 2, 2024; Published: October 4, 2024.

DOI: 10.15376/biores.19.4.8894-8911

APPENDIX

Supplemental Tables

Table S1a. Distance from Cavity to Radial Micro Zones in Corner Direction

Sample	C1 (mm)						
Sample	peripheral	transitional	central	inner			
n-1	5.55	5.29	4.33	2.44			
n-2	5.74	5.38	3.81	2.10			
n-3	7.05	6.82	5.21	2.11			

Sample		C2 (mm)						
Sample	peripheral	transitional	central	inner				
n-1	5.31	5.04	4.09	2.43				
n-2	5.80	5.27	4.03	2.11				
n-3	5.99	5.57	4.28	2.11				

Sample	C3 (mm)					
Sample	peripheral	transitional	central	inner		
n-1	5.22	4.94	3.56	2.45		
n-2	5.84	5.32	4.00	2.11		
n-3	6.09	5.57	4.63	2.11		

Sample		C4 (mm)					
	peripheral	transitional	central	inner			
n-1	5.32	4.92	4.24	2.45			
n-2	5.91	3.86	2.82	2.10			
n-3	6.19	5.78	4.28	2.11			

C = corner region

Table S1b. Distance from Cavity to Micro Areas of Sides

Sample		S1 (mm)		
Sample	peripheral	transitional	central	inner
n-1	4.95	4.65	3.91	2.44
n-2	5.40	5.07	3.84	2.11
n-3	5.48	5.30	3.76	2.10

Sample		S2 (mm)		
Sample	peripheral	transitional	central	inner
n-1	4.66	4.47	3.42	2.43
n-2	4.83	4.58	3.75	2.11
n-3	5.55	4.96	4.00	2.11

Sample		S3 (mm)		
Gample	peripheral	transitional	central	inner
n-1	5.10	4.74	3.62	2.43
n-2	4.99	4.64	3.51	2.11
n-3	5.61	5.20	3.92	2.11

Sample		S4 (mm))	
Sample	peripheral	transitional	central	inner
n-1	4.57	4.26	3.46	2.43
n-2	4.69	4.44	3.17	2.10
n-3	5.82	5.18	3.97	2.11

S = side region

Table S2a. Analysis Results of Fibre Length

Circumferential	Fibre Length (µm)							
region	Peripheral	Transitional	Central	Inner	Average	SD	P value	
c1	1375.5	1710.1	1591.5	1116.1	1710.1	46.52778	5.47*10 ⁻²¹	
						915		
s1	1359.4	1589.1	1369.6	1112.5	1810.0	50.73444	2.04*10 ⁻¹²	
						886		
c2	1291.3	1810.0	1772.9	1033.2	1824.4	41.44667	9.5*10 ⁻³⁶	
						333		
s2	1226.6	1446.2	1585.0	1077.1	1619.5	68.31820	2.26*10 ⁻¹⁷	
						887		
c3	1406.2	1824.4	1800.7	1242.4	1589.1	49.07987	3.53*10 ⁻²⁴	
						384		
s3	1485.1	1848.7	1583.0	1201.0	1446.2	47.49978	4.13*10 ⁻¹⁸	
						983		
c4	1331.1	1619.5	1661.4	1216.7	1848.7	57.96374	4.26*10 ⁻¹¹	
						293		
s4	1294.4	1711.7	1542.8	1164.8	1711.7	48.42378	1.97*10 ⁻¹⁹	
						344		

C = corner site, S = side site, SD = Standard Deviation

Table S2b. Analysis Results of Fibre Width

Circumferential	Fibre width (µm)						
region	Peripheral	Transitional	Central	Inner	Average	SD	P value
c1	13.5	15.0	14.9	12.9	13.5	0.22	4.99*10 ⁻⁸
						9202	
s1	16.4	14.7	15.4	13.5	16.4	0.21	5.1*10 ⁻¹⁸
						1575	
c2	13.2	15.8	14.1	12.6	13.2	0.27	7.1*10 ⁻⁵
						2545	
s2	13.6	17.1	14.3	13.4	13.6	0.23	1.21*10 ⁻⁶
						6659	
c3	14.4	17.1	14.2	12.5	14.4	0.25	2.92*10 ⁻¹³
						8233	
s3	13.8	15.3	14.8	13.7	13.8	0.23	2.47*10 ⁻⁶
						1276	
c4	14.1	15.9	13.6	12.5	14.1	0.23	0.06
						9153	
s4	14.3	15.8	14.9	13.3	14.3	0.31	8.16*10 ⁻⁷
						0914	

Table S2c. Analysis Results of Fibre Wall Thickness

Circumferential	Wall Thickness (μm)							
region	Peripheral	Peripheral	Transitional	Central	Inner	Average	SD	P value
c1	2.7	12.3	16.2	15.6	12.4	12.3	0.24494	2.93*10 ⁻¹⁸
s1	3.0	13.3	14.3	13.7	12.7	13.3	0.408271	2.18*10 ⁻¹⁵
c2	2.4	13.6	15.7	14.6	11.8	13.6	0.468872	0.0012
s2	2.4	15.0	16.6	13.9	11.7	15.0	0.552533	7.13*10 ⁻¹⁴
c3	1.9	10.9	15.5	12.9	12.0	10.9	0.282108	2.16*10 ⁻⁸
s3	2.6	16.7	15.0	15.5	14.0	16.7	0.480081	0.0149
c4	2.5	11.2	16.4	16.3	13.2	11.2	0.201792	1.6*10 ⁻⁹
s4	1.5	6.6	15.8	15.8	10.9	6.6	0.284779	1.01*10 ⁻⁶

C = corner region, S = side region, SD = Standard Deviation

Table S2d. Analysis Results of Fibre Lumen Diameter

Circumferential	Lumen Diameter (µm)						
region	Transitional	Central	Inner	Average	SD	P value	
c1	3.3	2.5	2.1	3.3	0.131505	1.7*10 ⁻²⁷	
s1	5.8	2.4	2.4	3.8	0.547282	0.0258	
c2	3.1	2.6	2.6	3.1	0.128875	6.8*10 ⁻³⁰	
s2	3.3	2.4	2.0	3.3	0.151319	1.09*10 ⁻²⁹	
с3	3.2	2.3	2.4	3.2	0.145083	1.51*10 ⁻²⁵	
s3	3.0	3.4	2.7	3.0	0.171416	0.0004	
c4	3.5	2.7	2.3	3.5	0.167868	6.97*10 ⁻⁴⁷	
s4	2.7	2.6	1.9	2.7	0.134085	1.85*10 ⁻⁴⁰	

Table S3. Difference of Fibre Characteristics in Circumferential Regions at Each Radial Micro Zone

Radial zone		P-value							
Radiai Zone	FL	FW	WT	LD					
Peripheral	0.000106	3.18*10 ⁻¹⁹	7.66*10 ⁻⁵⁴	9.81*10 ⁻¹²					
Transitional	4.09*10 ⁻¹⁰	4.65*10 ⁻⁰⁷	6.19*10 ⁻⁰⁶	1.03*10 ⁻¹⁷					
Central	6.51*10 ⁻⁰⁹	0.007068	1.58*10 ⁻²⁰	6.24*10 ⁻⁰⁷					
Inner	0.000921	0.000784	1.67*10 ⁻¹¹	0.000693					

FL = fibre length, FW = fibre width, WT = fibre wall thickness, LD = fibre lumen diameter